Title

Cyclooxygenase-derived proangiogenic metabolites of epoxyeicosatrienoic acids

Permalink

https://escholarship.org/uc/item/35d7203r

Journal

Proceedings of the National Academy of Sciences of the United States of America, 114(17)

ISSN

0027-8424

Authors

Rand, Amy A
Barnych, Bogdan
Morisseau, Christophe
et al.

Publication Date

2017-04-25

DOI

10.1073/pnas.1616893114

Peer reviewed

Cyclooxygenase-derived proangiogenic metabolites of epoxyeicosatrienoic acids

Amy A. Rand[a,b], Bogdan Barnych[a,b], Christophe Morisseau[a,b], Tomas Cajka[c], Kin Sing Stephen Lee[a,b], Dipak Panigrahy[d,e], and Bruce D. Hammock[a,b,1]

[a]Department of Entomology and Nematology, University of California, Davis, CA 95616; [b]UC Davis Comprehensive Cancer Center, University of California, Davis, CA 95616; [c]West Coast Metabolomics Center, UC Davis Genome Center, University of California, Davis, CA 95616; [d]Center for Vascular Biology Research, Beth Israel Deaconess Medical Center, Harvard Medical School, Boston, MA 02115; and [e]Department of Pathology, Beth Israel Deaconess Medical Center, Harvard Medical School, Boston, MA 02115

Arachidonic acid (ARA) is metabolized by cyclooxygenase (COX) and cytochrome P450 to produce proangiogenic metabolites. Specifically, epoxyeicosatrienoic acids (EETs) produced from the P450 pathway are angiogenic, inducing cancer tumor growth. A previous study showed that inhibiting soluble epoxide hydrolase (sEH) increased EET concentration and mildly promoted tumor growth. However, inhibiting both sEH and COX led to a dramatic decrease in tumor growth, suggesting that the contribution of EETs to angiogenesis and subsequent tumor growth may be attributed to downstream metabolites formed by COX. This study explores the fate of EETs with COX, the angiogenic activity of the primary metabolites formed, and their subsequent hydrolysis by sEH and microsomal EH. Three EET regioisomers were found to be substrates for COX, based on oxygen consumption and product formation. EET substrate preference for both COX-1 and COX-2 were estimated as 8,9-EET > 5,6-EET > 11,12-EET, whereas 14,15-EET was inactive. The structure of two major products formed from 8,9-EET in this COX pathway were confirmed by chemical synthesis: *ct*-8,9-epoxy-11-hydroxy-eicosatrienoic acid (*ct*-8,9-E-11-HET) and *ct*-8,9-epoxy-15-hydroxy-eicosatrienoic acid (*ct*-8,9-E-15-HET). *ct*-8,9-E-11-HET and *ct*-8,9-E-15-HET are further metabolized by sEH, with *ct*-8,9-E-11-HET being hydrolyzed much more slowly. Using an s.c. Matrigel assay, we showed that *ct*-8,9-E-11-HET is proangiogenic, whereas *ct*-8,9-E-15-HET is not active. This study identifies a functional link between EETs and COX and identifies *ct*-8,9-E-11-HET as an angiogenic lipid, suggesting a physiological role for COX metabolites of EETs.

omega-6 fatty acids | epoxyeicosatrienoic acids | metabolism | cyclooxygenase | angiogenesis

Arachidonic acid (ARA) is an omega-6 fatty acid that is metabolized by three major classes of enzymes, cyclooxygenases (COXs), lipoxygenases, and cytochrome P450s (CYPs), to produce an array of biologically active metabolites (1–3). The CYP pathway transforms ARA into four epoxyeicosatrienoic acids (EETs) in addition to hydroxylated metabolites (1). EETs have several biological actions, and are considered antihypertensive, antiinflammatory, neuroprotective, cardioprotective, and analgesic (4). EETs also play a role in angiogenesis (5–10), the formation of new blood vessels from preexisting vessels that is important for many physiological and pathological processes, including cancer (11).

EETs can enhance tumor growth and metastasis through their angiogenic activity (12); however, this activity is transient due to their metabolic instability. EETs are further metabolized by epoxide hydrolases (EHs), primarily soluble epoxide hydrolase (sEH), to their corresponding diols (4, 13), which are generally not biologically active (14) (Fig. 1*A*). Inhibition of sEH prolongs EET biological activity, potentiating their angiogenic activity, leading to increased tumor growth and metastasis in some systems (12, 15) (Fig. 1*B*).

ARA can also be metabolized by COX to form proangiogenic and proinflammatory prostaglandins (16). Angiogenesis stimulated from exposure to ARA can be mediated using COX inhibitors, which suppress the formation of prostaglandins (16). Compared with sEH inhibitors, COX inhibitors (i.e., the COX-2 selective inhibitor celecoxib) suppress angiogenesis and tumor growth, whereas sEH inhibitors alone tend to stimulate these responses in animals on a high–omega-6 fat diet (15). It was therefore surprising that administration of a dual sEH and COX inhibitor led to an antiangiogenic and anticancer response more pronounced than administration of these inhibitors alone (15). Similarly, when a COX (celecoxib) and sEH inhibitor (trans-4-[4-(3-adamantan-1-ylureido)cyclohexyloxy]benzoic acid; *t*-AUCB) were administered simultaneously to mice, tumor growth was much more inhibited than administration of the same two inhibitors alone, as shown in Fig. 1*B* (15). These results indicate that coincubation with a COX and sEH inhibitor produces a synergistic effect, better at inhibiting primary tumor growth and metastasis through the suppression of cancer angiogenesis. This suggests that EETs, whose levels are controlled by sEH, are metabolized by COX to form angiogenic, protumorigenic products that enhance the procancer response of EETs. Inhibiting COX decreases their formation and activity, as observed in a previous study (16).

The link between the COX and sEH pathways that stimulates angiogenesis and tumor progression may be explained by a relatively unexplored pathway associated with EET metabolism. Although EETs are primarily metabolized by sEH, a few studies have observed that the 5,6-EET and 8,9-EET are substrates for COX-1 (17, 18) and COX-2 (19). The COX metabolites of EETs have largely undefined biological activity, yet Homma et al. determined that the *ct*-8,9-epoxy-11-hydroxy-eicosatrienoic acid (*ct*-8,9-E-11-HET) metabolite is a renal vasoconstrictor and potent mitogen, approximately three orders of magnitude more potent than its parent, 8,9-EET (20). This provides evidence that EETs undergo metabolism by COX, forming metabolites that have greater activity than their parent compounds. If these COX metabolites are also angiogenic, this activity may be mitigated with COX inhibitors.

Significance

This study furthers our understanding of epoxyeicosatrienoic acid metabolism by cyclooxygenase (COX) enzymes as a physiologically relevant metabolic pathway, producing signaling molecules that are angiogenic. It explains, in part, why inhibiting the soluble epoxide hydrolase (sEH) in some systems is angiogenic whereas combining sEH inhibition with COX inhibition is dramatically antiangiogenic, which in turn may suppress tumor growth.
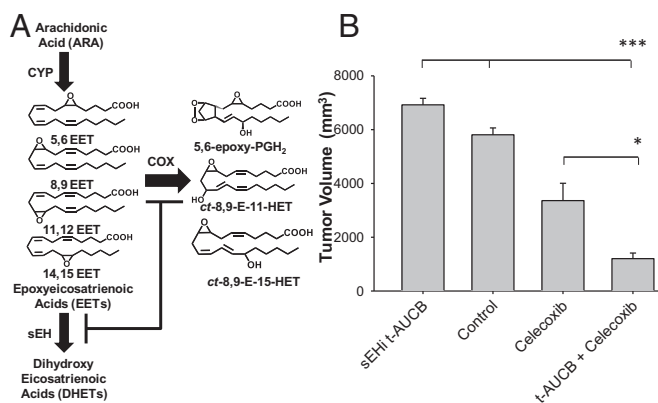
Fig. 1. ARA is metabolized by CYP to form metabolites that enhance angiogenesis and tumor growth. (*A*) EETs are metabolized by sEH to less active dihydroxyeicosatrienoic acids and by COX to hydroxy-EETs (*ct*-8,9-E-11-HET and *ct*-8,9-E-15-HET) and prostaglandin analogs (5,6-epoxy-PGH₂), regulators of mitogenesis, vasoactivity, and angiogenesis. sEH inhibition preserves and increases EET levels, thought responsible for angiogenesis and increased tumor growth, yet COX inhibition blocks this activity. (*B*) Tumor volume is altered by the selective COX-2 inhibitor celecoxib and an sEH inhibitor (sEHi *t*-AUCB). Treatment of primary Lewis lung carcinoma tumors in mice with *t*-AUCB (10 mg/kg/d) enhanced growth. By contrast, treatment with celecoxib (30 mg/kg/d) suppressed tumor growth. Combined treatment of celecoxib with sEHi (3 mg/kg/d) was most effective at reducing tumor growth, possibly through blocked production of the EET COX metabolites. Adapted with permission from ref. 15. Results are expressed as mean ± SD (*n* = 4 or 5 mice per group), *P < 0.05, ***P < 0.001.

Here we examine whether EETs (5,6-, 8,9-, 11,12-, and 14,15-EET) can be further metabolized by both COX isozymes. Reactivity for each substrate was determined by measuring oxygen consumption and elucidating products using LC-QToF-MS. The 8,9-EET was turned over most rapidly by COX, forming two abundant products: *ct*-8,9-E-11-HET and *ct*-8,9-epoxy-15-hydroxy-eicosatrienoic acid (*ct*-8,9-E-15-HET). These products were determined to be substrates for EHs, by calculating their kinetics subsequent to quantification of their hydration products. We also assess the angiogenic potential for *ct*-8,9-E-11-HET and *ct*-8,9-E-15-HET. Overall, this study further defines an alternative metabolic fate for the EETs with the COX enzymes, forming products that influence cancer angiogenesis.

Results and Discussion

Oxygenation of ARA and EETs by Cyclooxygenases. An oxygen electrode was used to measure oxygen uptake to determine whether the EET regioisomers were substrates for COX, and to compare their relative affinities with respect to the known COX-1 and COX-2 substrate ARA. Because oxygen is required as a cosubstrate for COX, we could determine whether or not each EET regioisomer is a COX substrate by examining the amount of oxygen consumption for EET incubations with COX-1 and COX-2. As shown in *SI Appendix*, Fig. S1, 5,6-, 8,9-, and to a lesser extent 11,12-EET were substrates in the presence of both enzymes, yielding measurable oxygen consumption over 25 s at 50 μM. 5,6-EET, reported to be a COX substrate (18, 19), noticeably reacted with COX-1 and COX-2 at concentrations ranging between 15 and 50 μM (*SI Appendix*, Fig. S2). Compared with 5,6-EET, which is metabolized by COX through the same mechanism as ARA to form an endoperoxide prostaglandin analog, the epoxide position in 8,9-EET blocks endoperoxide formation and instead forms monohydroxyl products on C-11 or C-15. These products are *ct*-8,9-E-11-HET or *ct*-8,9-E-15-HET (17). Kinetic plots for 8,9-EET with COX-1 and COX-2 are presented in Fig. 2, and K_M and V_m values for 8,9-EET and ARA can be found in Table 1. The K_Ms obtained from these experiments for ARA reacting with COX-1 and COX-2 were similar to

literature values (independent *t* test, *P* > 0.05) (21). Likewise, K_M values for 8,9-EET with COX-1 and COX-2 are not significantly different from the ARA K_Ms, indicating that both substrates have similar affinities for both enzymes. All values obtained for V_m also showed no significant difference. 11,12-EET gave rates that were so low that the kinetic constants could not be calculated based on the response curves, and 14,15-EET showed no apparent reaction with COX-1 or COX-2 (*SI Appendix*, Figs. S3 and S4).

With respect to the enzymatic mechanism, epoxides placed at the 11,12 and 14,15 positions may alter the substrate orientation within the enzyme, limiting apparent reactivity. COX first catalyzes oxygenation by abstracting the substrate's 13-pro*S*-hydrogen, generating a radical with maximal electron density at C-11 and C-15, where oxygen then adds to form a peroxyl radical (22). Epoxides placed in either of these locations may limit the initial abstraction rate and addition of oxygen, compared with epoxides placed further from the initial catalytic C-13 (i.e., 5,6- and 8,9-EET). 14,15-EET was least active compared with the other regioisomers, possibly due to the epoxide proximity to the ω-end of the fatty acid. Because the ω-end resides within a channel at the top of the COX active site, substrates with substituents closer to the ω-end may further limit COX activity through added steric hindrance within this channel. For example, adding bulky substitutions within this channel has been shown to inhibit oxidation of ARA (23).

Product Studies of EETs with COX. It was evident from the oxygraph kinetics that the 5,6-, 8,9-, and less so the 11,12-EETs were active substrates for COX. This was subsequently confirmed by identifying the products (or lack thereof) formed by the kinetic reactions, using LC-QToF-MS. As expected, 5,6-EET metabolized to form its endoperoxide prostaglandin-like product (epoxy-PGH₂, *m/z* 367.2121), confirming its activity with COX-1 and COX-2 (Fig. 3). Signal intensity of this product not only depended on the presence of enzyme in the reaction but also dramatically decreased in the presence of the COX inhibitor ibuprofen, indicating this product resulted from a functioning COX enzyme rather than a nonenzymatic-dependent reaction.

8,9-EET was metabolized by COX-1 and COX-2 to form two products having an accurate mass of *m/z* 335.2228, corresponding to the mass of the *ct*-8,9-E-HET products, as has previously been observed to form with COX-1 (17). Structure assignment for both was done by MS/MS fragmentation. *SI Appendix*, Fig. S5 shows the fragment ions *m/z* 235.1425 and 127.0790 from the molecular ion (*m/z* 335.2218). This represented cleavage between the C–C bond both α and β from a 15-hydroxyl group, corresponding to the *ct*-8,9-E-15-HET product. The MS/MS spectrum of the second 8,9-EET COX product supports the *ct*-8,9-E-11-HET structure, because the bond is fragmented α to an
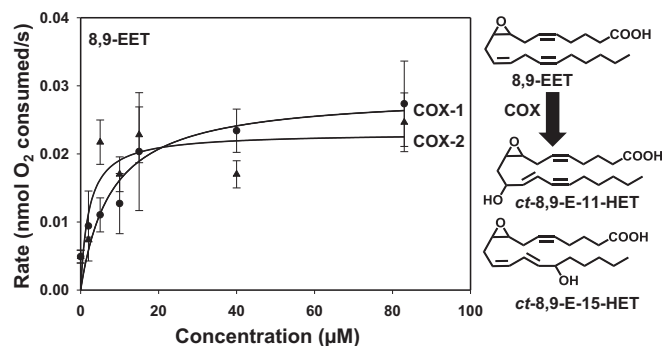

Fig. 2. Michaelis–Menten plots for oxygen consumption in the presence of 8,9-EET with COX-1 and COX-2 ([COX]_final, 5 μg/mL). (*A*) 8,9-EET oxygenation with COX-1 and COX-2 to form *ct*-8,9-E-11-HET and *ct*-8,9-E-15-HET. Results are expressed as mean ± SEM (*n* = 3 or 4 samples). (*B*) The 8,9-EET structure as it is converted to *ct*-8,9-E-11-HET and *ct*-8,9-E-15-HET.

Table 1. Kinetic values comparing ARA and 8,9-EET for the enzymes ovine cyclooxygenase 1 and human cyclooxygenase 2

Enzyme	Substrate	Product	K_M, µM	V_m, pmol·min^{-1}	k_{cat}, s^{-1}	k_{cat}/K_M, µM^{-1}·s^{-1}
COX-1	ARA	O$_2$ cons.	2.6 ± 1.0 (3.4 ± 0.6)	0.35 ± 0.04	0.91 ± 0.01	0.35 ± 0.10
	8,9-EET	O$_2$ cons.	7.9 ± 3.2	0.52 ± 0.06	0.67 ± 0.08	0.09 ± 0.02
COX-2	ARA	O$_2$ cons.	2.0 ± 0.9 (6.1 ± 0.6)	0.77 ± 0.08	2.0 ± 0.22	1.0 ± 0.33
	8,9-EET	O$_2$ cons.	2.1 ± 1.7	0.41 ± 0.06	1.1 ± 0.16	0.52 ± 0.33

Results are average ± SEM ($n = 3$ or 4). ARA kinetic values taken from the literature are in parentheses (21). The relatively high rate of 8,9-EET metabolism by COX-1 and COX-2 determined by oxygen consumption (cons.) correlates with the high rate of ct-8,9-E-11-HET formed.

11-hydroxyl group to produce m/z 183.1014, which then loses a water molecule (m/z 165.0926), followed by carbon dioxide (m/z 121.1032). Independent synthesis of ct-8,9-E-11-HET and ct-8,9-E-15-HET confirmed the identity of the two products by cochromatography, and matching LC retention times and MS/MS spectra with the metabolites (*SI Appendix*, Figs. S6 and S7).

11,12-EET was not metabolized rapidly enough to provide reliable kinetic information using the oxygraph. Nevertheless, its reaction with COX-1 and COX-2 formed products that were all inhibited by celecoxib, indicating that the chromatographic signals were not simply background noise. One of the products was converted to a triol (m/z 353.2328) by sEH (25 µg/mL), demonstrating the presence of at least one 11,12-E-HET product (*SI Appendix*, Fig. S8). All products also had identical masses and similar retention times to the 8,9-E-HETs, further evidence supporting these products as 11,12-E-HET isomers. Although the exact regioisomers of the 11,12-E-HET products are uncertain, we have determined that 11,12-EET is a weak substrate for COX-1 and stronger for COX-2, estimated from relative peak area. 14,15-EET failed to react with these enzymes, as evidenced from its lack of oxygen consumption and product formation.

8,9-E-HET Hydrolysis. Based on kinetic and product studies, 8,9-EET formed the most abundant COX products compared with other EET regioisomers. Therefore, we synthesized these products to understand their metabolic fate with EH enzymes. To confirm that 8,9-E-HET products are substrates for sEH and microsomal EH (mEH), we developed an analytical method for their hydrolytic products to determine kinetic constants (K_M and k_{cat}) (Fig. 4 for sEH and *SI Appendix*, Fig. S9 for mEH). These constants were compared with the known EH substrate 8,9-EET (Table 2 for sEH and *SI Appendix*, Table S2 for mEH). All 8,9-E-HETs were substrates of both EHs, with comparable k_{cat}/K_M values for each enzyme. For sEH, the K_M and V_m constants for 8,9-EET were higher than for the 8,9-E-HET products. However, the resulting k_{cat}/K_M values for all four compounds were similar, indicating that at physiological concentrations, sEH hydrolyzes these four oxylipids in a similar fashion regardless of the presence and location of the hydroxyl group. For mEH, an enzyme shown primarily to act on xenobiotic epoxides but that also can metabolize EETs, especially 8,9-EET (4), the k_{cat}/K_M value for 8,9-EET was at least two orders of magnitude higher than for the 8,9-E-HETs, with ct-8,9-E-15-HET being catalyzed 10-fold more than both 8,9-E-11-HET isomers. In this case, the hydroxyl group drastically lowers the enzymatic conversion rate so that the substrates may actually be binding to the enzyme, resulting in slow turnover. However, preliminary inhibition data showed that at high concentration (100 µM) the 8,9-E-HETs are no better at inhibiting mEH activity on a reporting substrate (*cis*-stilbene oxide 50 µM) than 8,9-EET (98% inhibition); ct-8,9-E-11-HET, tt-8,9-E-11-HET, and ct-8,9-E-15-HET gave 65, 71, and 95% mEH inhibition, respectively. Regardless, the slower kinetic turnover of 8,9-E-HETs by mEH may be important in tissues having higher levels of mEH, such as in some regions in the brain where sEH is absent (24, 25). In summary, 8,9-EET has similar turnover with sEH and mEH, whereas the 8,9-E-HETs are primarily substrates for sEH. This may be important for regulating

angiogenesis, because sEH is expressed in endothelial cells, unlike other EHs (26, 27). Inhibiting sEH has major effects on enhancing EET biological activity, including angiogenesis.

Matrigel Plug Assay. Angiogenesis is a complex process that involves proliferation and migration of endothelial cells to form new capillary vessels (28). Although highly regulated under normal physiological conditions, many diseases result in unregulated
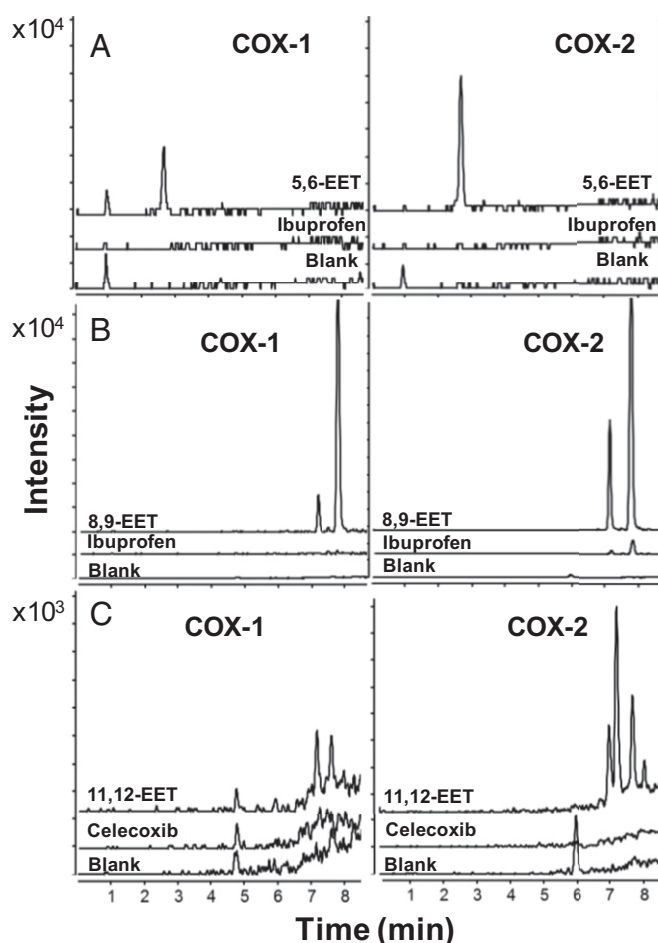
Fig. 3. EET products formed after reaction with COX-1 and COX-2, measured by HPLC-QToF-MS. (*A*) Intensity of the ion selective for 5,6-epoxy-PGH$_2$ (m/z 367.2121). (*B*) Intensity of the ion selective for 8,9-EET COX-1 and COX-2 products (m/z 335.2228). The larger peak is identified as ct-8,9-E-11-HET and the smaller as ct-8,9-E-15-HET. (*C*) Intensity of the ion selective for 11,12-EET COX-1 and COX-2 products (m/z 335.2228). Products were only observed in the chromatographs associated with substrate in the presence of either COX enzyme, inhibited with either ibuprofen or celecoxib, and absent in the blank chromatographs (without substrate).
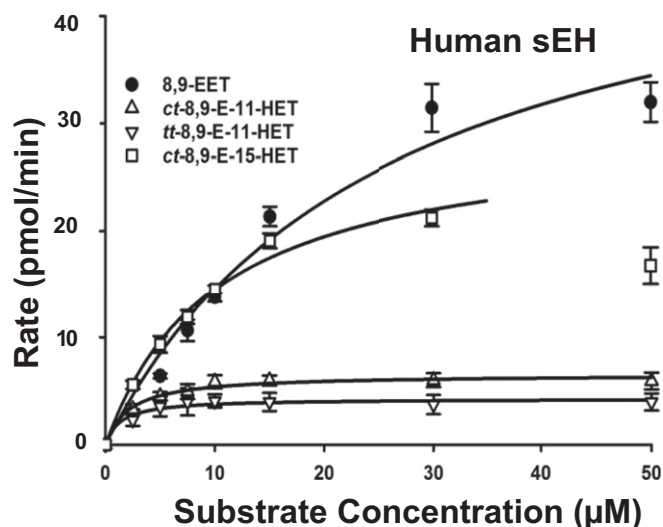
Fig. 4. Rate vs. substrate Michaelis–Menten plots for 8,9-EET, *tt*-8,9-E-11-HET, *ct*-8,9-E-11-HET, and *ct*-8,9-E-15-HET with human sEH ([sEH]$_{final}$, 0.1 μM) in Na$_3$PO$_4$ buffer (0.1 M, pH 7.4, containing 0.1 mg/mL BSA) at 37 °C. Results are expressed as average $\pm$ SEM ($n = 6$).

angiogenesis, including arthritis, diabetic retinopathy, cutaneous gastric ulcers, and cancer (28). EETs are endothelial mitogens and activate several signaling pathways that promote angiogenesis (9, 10, 29), tumor growth, and metastasis (12). Because the tumorigenic activity attributed to EETs is suppressed by COX inhibitors, it raises the possibility that COX metabolites of EETs may also be angiogenic.

We determined whether the *ct*-8,9-E-11-HET and *ct*-8,9-E-15-HET products of 8,9-EET were angiogenic using the in vivo Matrigel plug assay, which measures angiogenesis within an s.c. implanted plug rather than the whole animal. Using this assay, we could compare the effect of EETs and their 8,9-E-HET COX products on cell infiltration and the total number of cells within each plug, extent of extravascular red blood cells (hemorrhage), and number of microvessels (Fig. 5). The VEGF/FGF positive control group had the most effect at producing a large amount of cell infiltration and number of cells, which led to the formation of intact capillaries observed from CD31 staining (*SI Appendix*, Fig. S10). VEGF and FGF are both crucial factors in the development of blood vessels and induce angiogenesis through distinct pathways (30) yet synergize to enhance vessel formation (31). The presence of these growth factors also is associated with EET mitogenesis and angiogenesis. VEGF induces CYP2C8 expression, resulting in increased EET levels in endothelial cells (29), and incubation of 14,15-EET induces expression of FGF-2 in a Src/P13K-Akt–dependent manner in human dermal microvascular endothelial cells (32). In this study, the EET mixture increased the amount of cell infiltration, fourfold more than the vehicle control (Fig. 5A), but the change induced by the mixture was not significant for the other parameters. 8,9-EET had a significant amount of cell infiltration, total cells (primarily endothelial cells and fibroblasts), and microvessels, three-, two-, and

sixfold more than the vehicle control, respectively (Fig. 5 A, C, and D). The hemorrhage variation of 8,9-EET was high (Fig. 5B), therefore its level was not significant with respect to the control.

The lack of significance in the hemorrhage area (Fig. 5B) for 8,9-EET may be due to the variability of the response. Although previous studies have never quantified the amount of hemorrhage with respect to EETs, a few studies have measured increased total hemoglobin after 14,15-EET (9, 32) and 11,12-EET (33) administration. In these cases, there was less variability than the hemorrhage response in this study. One major factor controlling the red blood cell infiltration within the gel plugs is the concentration of heparin, a proangiogenic agent required to stabilize FGF (34). The magnitude of angiogenesis increases with heparin concentration, but heparin may also lead to greater hemorrhage. In these previous studies measuring total hemoglobin after EET administration, the heparin concentration was not reported. It is possible that reducing the amount of heparin may provide less variable results, although it has been reported that heparin at 40 U/mL produced the most consistent results with respect to the FGF angiogenic response (34). In this study, all groups had equal heparin concentration (40 U/mL). Therefore, the large hemorrhage variability may be due to 8,9-EET alone (although interactions between EETs and heparin are not well-understood).

Similar to the EETs, *ct*-8,9-E-11-HET significantly enhanced the amount of cell infiltration and total cell number within each Matrigel plug, with respective values of 2.5- and 3-fold more than the vehicle control (Fig. 5 A and C). The migration and proliferation also led to a 4.5-fold increase in microvessels (Fig. 5D). This demonstrates that *ct*-8,9-E-11-HET angiogenic activity may synergize with the activity observed for the EETs. COX inhibition with celecoxib may reduce angiogenesis and the protumorigenic effects of EETs, at least in part, by blocking formation of *ct*-8,9-E-11-HET.

Although EET angiogenic activity may be enhanced through metabolism by COX to form *ct*-8,9-E-11-HET, the cell signaling pathways that promote the angiogenic activity of *ct*-8,9-E-11-HET are currently unknown. There are notable differences between the *ct*-8,9-E-11-HET group and others in the gross morphology of the Matrigel plugs, all of which were very fragile and had large areas of hemorrhage (Fig. 5G). H&E staining of Matrigel sections showed marked presence of extravascular RBCs and many hematomas (*SI Appendix*, Fig. S11). The extensive hemorrhaging, 17-fold more than the vehicle control, suggests formation of unstable neovessels. Unstable neovessels resulting in excessive hemorrhage in Matrigel plugs was also previously observed from platelet inhibition (35). Platelets preferentially adhere and stabilize newly formed angiogenic vessels (35). *ct*-8,9-E-11-HET may inhibit platelets or other stabilizing factors, leading to an angiogenic response that includes formation of weak blood vessels. EETs, particularly 11,12- and 14,15-EET, reduce platelet aggregation through membrane hyperpolarization and enhanced expression and activity of endothelial fibrolytic enzymes (36), suggesting a similar and potentially greater interaction between *ct*-8,9-E-11-HET and platelets, reducing endothelial stability that leads to hemorrhage, although elucidating this relationship obviously warrants further research.

The hemorrhaging was also coupled with an inflammatory infiltrate made up of leukocytes in plugs treated with *ct*-8,9-E-11-HET (*SI Appendix*, Fig. S12). *ct*-8,9-E-11-HET may be a stimulator of inflammatory angiogenesis, due to the presence of these

Table 2. Kinetic constants of recombinant purified human sEH for 8,9-EET, *tt*-8,9-E-11-HET, *ct*-8,9-E-11-HET, and *ct*-8,9-E-15-HET

Enzyme	Substrate	Product	K_m, μM	V_m, pmol·min^{-1}	k_{cat}, s^{-1}	k_{cat}/K_m, μM^{-1}·s^{-1}
sEH	8,9-EET	8,9-DHET	26 ± 1	52 ± 7	$(5.6 \pm 0.3) \times 10^{-1}$	$(2.2 \pm 0.1) \times 10^{-2}$
	tt-8,9-E-11-HET	*tt*-8,9,11-THET	1.4 ± 0.5	4.3 ± 0.2	$(4.6 \pm 0.3) \times 10^{-2}$	$(3.3 \pm 0.5) \times 10^{-2}$
	ct-8,9-E-11-HET	*ct*-8,9,11-THET	2.2 ± 0.4	6.5 ± 0.2	$(7.0 \pm 0.3) \times 10^{-2}$	$(3.2 \pm 0.4) \times 10^{-2}$
	ct-8,9-E-15-HET	*ct*-8,9,15-THET	10 ± 2	30 ± 2	$(3.2 \pm 0.2) \times 10^{-1}$	$(3.2 \pm 0.1) \times 10^{-2}$

Results are average $\pm$ SD ($n = 6$). Statistically significant differences were determined by the independent t test.
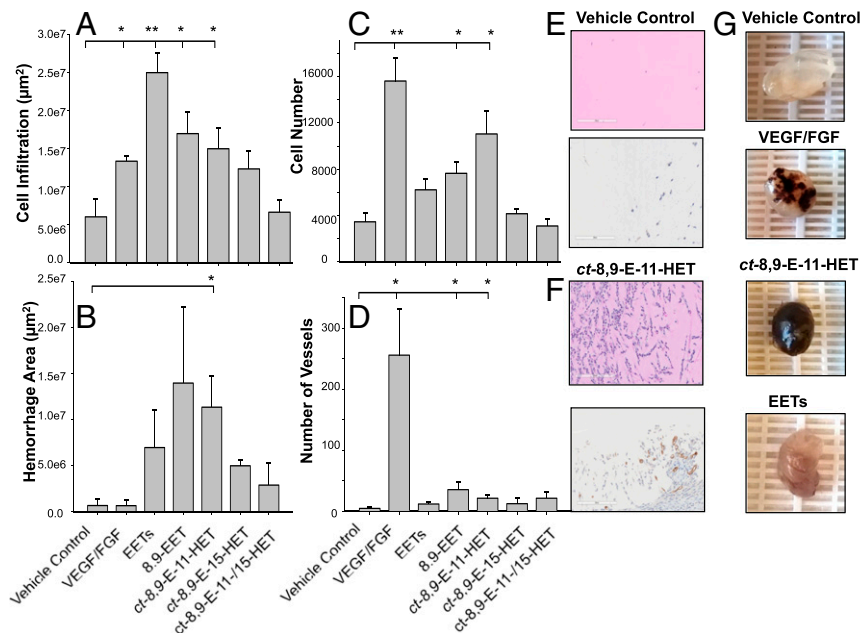
Fig. 5. (*A–D*) Effect of EETs and their 8,9-E-HET COX metabolites on (*A*) cell infiltration, (*B*) hemorrhage, (*C*) number of cells, and (*D*) number of microvessels within each Matrigel plug. For all parameters, quantitation was performed using Aperio ImageScope software (Leica Biosystems) after H&E or CD31 staining, and treatment groups were compared with a vehicle control group. Each bar represents the mean ± SEM ($n = 4$ to 6 mice per group), *$P \leq 0.05$, **$P \leq 0.01$. (*E*) Representative slides of vehicle control-treated Matrigel plug sections stained with H&E and CD31. (*F*) Representative slides of *ct*-8,9-E-11-HET–treated Matrigel plug sections stained with H&E and CD31 to show the contribution of cells (dark blue) and microvessels (dark brown) to blood vessel formation, respectively. Images were taken at 20× magnification. (Scale bars: *E* and *F*, 200 μm.) (*G*) Representative photographs of Matrigel plug gross morphology from mice injected with ethanol (vehicle control), VEGF and FGF, *ct*-8,9-E-11-HET, and the EET mixture.

inflammatory cells. Leukocyte infiltration has been observed in lipopolysaccharide-conditioned Matrigel, a model for inducing inflammatory angiogenesis (37). In this model, neutrophils invade and degrade the gel by creating clefts, followed by migrational macrophages. Growth factors such as VEGF and bFGF released by neutrophils and macrophages subsequently induce endothelial cell migration and tube formation, and the resulting angiogenesis is directly dependent upon leukocyte migration. This may explain why, despite the presence of hemorrhage, *ct*-8,9-E-11-HET still produced intact vessels, which formed through the presence of additional growth factors from the leukocytes.

By contrast to *ct*-8,9-E-11-HET, *ct*-8,9-E-15-HET and the combination of *ct*-8,9-E-11-HET and *ct*-8,9-E-15-HET were not significantly different from the vehicle control, suggesting some biological dependency on the position of the hydroxyl group, that *ct*-8,9-E-15-HET may not be a critical component for stimulating angiogenesis (Fig. 5 *A–D*). Using the purified enzymes described above, *ct*-8,9-E-11-HET forms ∼2- to 10-fold more than *ct*-8,9-E-15-HET, although formation of these products may be dependent on species, tissue, and cell type. Although the combination of *ct*-8,9-E-11-HET and *ct*-8,9-E-15-HET was expected to be angiogenic, given that *ct*-8,9-E-11-HET gave an effect on its own, this group did not produce any significant activity. *ct*-8,9-E-15-HET may be an antagonist to *ct*-8,9-E-11-HET, which acts to block or reduce the activity of *ct*-8,9-E-11-HET. Alternatively, because *ct*-8,9-E-11-HET and *ct*-8,9-E-15-HET together produced a total concentration of 100 μM and the level of *ct*-8,9-E-11-HET in this treatment was lower than the individual treatment, the activity of *ct*-8,9-E-11-HET might be below the detection limit of this assay.

Lipid treatments were at levels much higher than their reported nanomolar endogenous levels (38). The 100 μM concentration was chosen because EETs and 8,9-E-HETs are labile, and only dosed once within the 7-d treatment period. However, *ct*-8,9-E-11-HET may be angiogenic at endogenous levels based on its expected presence within endothelial cells. These cells are known to express high levels of CYPs, which form EETs that have diverse effects on the vasculature, including angiogenesis. For example,

overexpression of CYP2J2 in bovine aortic endothelial cells promotes cell proliferation, migration, and tube formation (39). COX-1 is constitutively expressed in most tissues, and therefore we might expect the formation of the 8,9-E-HET metabolites, because their formation by COX-1 was demonstrated in this study and others (17). The combination of COX-1 and COX-2 may lead to the highest levels of E-HETs formed, as we show EETs to be substrates for both enzymes. Under normal conditions, COX-2 is expressed at low or undetectable levels but becomes up-regulated by inflammatory, mitogenic, and physical stimuli (40). In addition, the expression of VEGF, a critical factor for angiogenesis, up-regulates COX-2, which may in turn increase endogenous levels of *ct*-8,9-E-11-HET that will promote angiogenesis (41).

In summary, we have explored the fate of EETs with COX, with particular attention to 8,9-EET and the angiogenic activity of its products. Although these products are substrates for sEH, inhibition of sEH may stabilize 8,9-E-HETs in circulation, leading to angiogenesis from increased levels of *ct*-8,9-E-11-HET, which may in turn promote tumor growth and metastasis.

Materials and Methods

Details of the experimental protocols are given in *SI Appendix, Materials and Methods*.

COX Activity Assay by Oxygen Consumption. A Hansatech Oxygraph Plus oxygen electrode system was used to measure the oxygen consumption involved in the activity of COX-1 and COX-2 with EETs (5,6- and 14,15-EET). Tris·HCl buffer [100 mM, pH 8.0, with 5 mM EDTA (USB)] was first added to the electrode chamber. Bovine hematin and phenol were then added to give final concentrations of 2 μM and 1 mM, respectively. This solution was warmed to 37 °C before adding COX-1 or COX-2 ([COX]$_{final}$ ∼5 μg/mL, determined by the bicinchoninic acid assay). Reactions were initiated by adding a solution of the epoxy fatty acid in 1:1 ethanol/Tris·HCl buffer through the central bore of the Oxygraph plunger, with final concentrations ranging from 0.1 to 80 μM. Oxygen consumption was followed until the rate before addition of substrate returned. The amount of ethanol was 0.8% of the total volume (300 μL). K_M and V_m for COX-1 and COX-2 with each substrate were

estimated by nonlinear regression to the Michaelis–Menten equation (SigmaPlot 11.0; Systat Software). Reactions were done with $n = 2$ to 4 replicates. Products from these reactions were analyzed using LC-QToF-MS, described in *SI Appendix, Materials and Methods*.

EH Kinetic Assay Conditions. Kinetic parameters for 8,9-EET, *tt*-8,9-E-11-HET, *ct*-8,9-E-11-HET, and *ct*-8,9-E-15-HET were determined under steady-state conditions using recombinant human sEH (95% pure) and mEH (80% pure). The E-HETs were first converted from their methyl ester to their carboxylic acid form using recombinant partially purified carboxylesterase 2 (CES 2) free of epoxide hydrolase activity. In glass tubes (10 × 75 mm), to 90 μL of a solution of CES 2 (27 μg/mL in Na_3PO_4 buffer (0.1 M, pH 7.4, containing 0.1 mg/mL BSA)], 1 μL substrates in DMSO ([S]$_f$ = 2.5 to 50 μM) was added and the mixture was incubated for 30 min at 37 °C. Each enzyme in Na_3PO_4 buffer ([sEH]$_f$ = 0.10 μg per tube; [mEH]$_f$ = 2.96 μg per tube) was then added (10 μL). The mixture was incubated for an additional 30 min at 37 °C. Reactions were quenched by adding 100 μL of methanol containing 0.4 μM *N*-cyclohexyl-*N′*-dodecanoic acid urea as an internal standard, used for its structural similarity to the measured analytes rather than its ability to inhibit sEH. The quantity of products formed, either 8,9-dihydroxyeicosatrienoic acid (8,9-DHET), 8,9,11-trihydroxyeicosatrienoic acid (8,9,11-THET), or 8,9,15-THET was determined by LC-MS/MS. Kinetic constants (K_M and V_m) were calculated by nonlinear fitting of the Michaelis–Menten equation (SigmaPlot 11.0). Reactions were done in hexaplicate ($n = 6$).

Matrigel Plug Assay. All procedures and animal care were performed in accordance with the protocols approved by the Institutional Animal Care and Use Committee of the University of California. Growth factor-reduced Matrigel (0.5 mL) at ≥9.2 mg/mL protein concentration was mixed with 20 U heparin and the following treatments: an EET mixture (5,6-, 8,9-, 11,12-, and 14,15-EET at a molar ratio of 1:1.1:1.6:2.2, respectively), 8,9-EET, *ct*-8,9-E-11-HET, *ct*-8,9-E-15-HET, and a 1:1 mixture of *ct*-8,9-E-11- and 15-HET. These treatments were dissolved in ethanol and added to each Matrigel mixture to give a final concentration of 100 μM with an ethanol volume no greater than 0.4%. There was also a positive control group that contained 200 ng/mL mouse VEGF 164 and 100 ng/mL mouse FGF-2, and a vehicle control group containing ethanol. The Matrigel mixtures were s.c. injected into the right abdominal area in C57BL/6 mice. After 6 d, animals were euthanized to dissect the Matrigel plugs, which were then sectioned and stained by the Center for Genomic Pathology Laboratory at the University of California, Davis.

Statistics. Group comparisons were carried out using the independent *t* test after evaluating the Levene's test for equality of variances using SPSS 24 software (IBM Analytics) or SigmaPlot 11.0. A *P* value ≤ 0.05 was considered statistically significant. Data are presented as mean ± SEM.

1. Zeldin DC (2001) Epoxygenase pathways of arachidonic acid metabolism. *J Biol Chem* 276:36059–36062.
2. Brash AR (1999) Lipoxygenases: Occurrence, functions, catalysis, and acquisition of substrate. *J Biol Chem* 274:23679–23682.
3. Smith WL, Garavito RM, DeWitt DL (1996) Prostaglandin endoperoxide H synthases (cyclooxygenases)-1 and -2. *J Biol Chem* 271:33157–33160.
4. Morisseau C, Hammock BD (2013) Impact of soluble epoxide hydrolase and epoxyeicosanoids on human health. *Annu Rev Pharmacol Toxicol* 53:37–58.
5. Cheranov SY, et al. (2008) An essential role for SRC-activated STAT-3 in 14,15-EET-induced VEGF expression and angiogenesis. *Blood* 111:5581–5591.
6. Fleming I (2001) Cytochrome p450 and vascular homeostasis. *Circ Res* 89:753–762.
7. Fleming I (2007) Epoxyeicosatrienoic acids, cell signaling and angiogenesis. *Prostaglandins Other Lipid Mediat* 82:60–67.
8. Panigrahy D, Greene ER, Pozzi A, Wang DW, Zeldin DC (2011) EET signaling in cancer. *Cancer Metastasis Rev* 30:525–540.
9. Medhora M, et al. (2003) Epoxygenase-driven angiogenesis in human lung microvascular endothelial cells. *Am J Physiol Heart Circ Physiol* 284:H215–H224.
10. Pozzi A, et al. (2005) Characterization of 5,6- and 8,9-epoxyeicosatrienoic acids (5,6- and 8,9-EET) as potent in vivo angiogenic lipids. *J Biol Chem* 280:27138–27146.
11. Folkman J (1995) Angiogenesis in cancer, vascular, rheumatoid and other disease. *Nat Med* 1:27–31.
12. Panigrahy D, et al. (2012) Epoxyeicosanoids stimulate multiorgan metastasis and tumor immune escape in mice. *J Clin Invest* 122:178–191.
13. Decker M, et al. (2012) EH3 (ABHD9): The first member of a new epoxide hydrolase family with high activity for fatty acid epoxides. *J Lipid Res* 53:2038–2045.
14. Newman JW, Morisseau C, Hammock BD (2005) Epoxide hydrolases: Their roles and interactions with lipid metabolism. *Prog Lipid Res* 44:1–51.
15. Zhang G, et al. (2014) Dual inhibition of cyclooxygenase-2 and soluble epoxide hydrolase synergistically suppresses primary tumor growth and metastasis. *Proc Natl Acad Sci USA* 111:11127–11132.
16. Wang D, Dubois RN (2010) Eicosanoids and cancer. *Nat Rev Cancer* 10:181–193.
17. Zhang JY, Prakash L, Yamashita K, Blair IA (1992) Regiospecific and enantioselective metabolism of 8,9-epoxyeicosatrienoic acid by cyclooxygenase. *Biochem Biophys Res Commun* 183:138–143.
18. Carroll MA, Balazy M, Margiotta P, Falck JR, McGiff JC (1993) Renal vasodilator activity of 5,6-epoxyeicosatrienoic acid depends upon conversion by cyclooxygenase and release of prostaglandins. *J Biol Chem* 268:12260–12266.
19. Moreland KT, et al. (2007) Cyclooxygenase (COX)-1 and COX-2 participate in 5,6-epoxyeicosatrienoic acid-induced contraction of rabbit intralobar pulmonary arteries. *J Pharmacol Exp Ther* 321:446–454.
20. Homma T, et al. (1993) Cyclooxygenase-derived metabolites of 8,9-epoxyeicosatrienoic acid are potent mitogens for cultured rat glomerular mesangial cells. *Biochem Biophys Res Commun* 191:282–288.
21. Prusakiewicz JJ, et al. (2007) Oxidative metabolism of lipoamino acids and vanilloids by lipoxygenases and cyclooxygenases. *Arch Biochem Biophys* 464:260–268.
22. Marnett LJ, Rowlinson SW, Goodwin DC, Kalgutkar AS, Lanzo CA (1999) Arachidonic acid oxygenation by COX-1 and COX-2. Mechanisms of catalysis and inhibition. *J Biol Chem* 274:22903–22906.

23. Rowlinson SW, Crews BC, Lanzo CA, Marnett LJ (1999) The binding of arachidonic acid in the cyclooxygenase active site of mouse prostaglandin endoperoxide synthase-2 (COX-2). A putative L-shaped binding conformation utilizing the top channel region. *J Biol Chem* 274:23305–23310.
24. Marowsky A, Burgener J, Falck JR, Fritschy J-M, Arand M (2009) Distribution of soluble and microsomal epoxide hydrolase in the mouse brain and its contribution to cerebral epoxyeicosatrienoic acid metabolism. *Neuroscience* 163:646–661.
25. Sura P, Sura R, Enayetallah AE, Grant DF (2008) Distribution and expression of soluble epoxide hydrolase in human brain. *J Histochem Cytochem* 56:551–559.
26. Fang X, et al. (2001) Pathways of epoxyeicosatrienoic acid metabolism in endothelial cells. Implications for the vascular effects of soluble epoxide hydrolase inhibition. *J Biol Chem* 276:14867–14874.
27. Decker M, Arand M, Cronin A (2009) Mammalian epoxide hydrolases in xenobiotic metabolism and signalling. *Arch Toxicol* 83:297–318.
28. Koch AE, et al. (1994) Vascular endothelial growth factor. A cytokine modulating endothelial function in rheumatoid arthritis. *J Immunol* 152:4149–4156.
29. Webler AC, et al. (2008) Epoxyeicosatrienoic acids are part of the VEGF-activated signaling cascade leading to angiogenesis. *Am J Physiol Cell Physiol* 295:C1292–C1301.
30. Giavazzi R, et al. (2003) Distinct role of fibroblast growth factor-2 and vascular endothelial growth factor on tumor growth and angiogenesis. *Am J Pathol* 162:1913–1926.
31. Kano MR, et al. (2005) VEGF-A and FGF-2 synergistically promote neoangiogenesis through enhancement of endogenous PDGF-B-PDGFRbeta signaling. *J Cell Sci* 118:3759–3768.
32. Zhang B, Cao H, Rao GN (2006) Fibroblast growth factor-2 is a downstream mediator of phosphatidylinositol 3-kinase-Akt signaling in 14,15-epoxyeicosatrienoic acid-induced angiogenesis. *J Biol Chem* 281:905–914.
33. Yan G, Chen S, You B, Sun J (2008) Activation of sphingosine kinase-1 mediates induction of endothelial cell proliferation and angiogenesis by epoxyeicosatrienoic acids. *Cardiovasc Res* 78:308–314.
34. Passaniti A, et al. (1992) A simple, quantitative method for assessing angiogenesis and antiangiogenic agents using reconstituted basement membrane, heparin, and fibroblast growth factor. *Lab Invest* 67:519–528.
35. Kisucka J, et al. (2006) Platelets and platelet adhesion support angiogenesis while preventing excessive hemorrhage. *Proc Natl Acad Sci USA* 103:855–860.
36. Sudhahar V, Shaw S, Imig JD (2010) Epoxyeicosatrienoic acid analogs and vascular function. *Curr Med Chem* 17:1181–1190.
37. Benelli R, et al. (2002) Neutrophils as a key cellular target for angiostatin: Implications for regulation of angiogenesis and inflammation. *FASEB J* 16:267–269.
38. Node K, et al. (1999) Anti-inflammatory properties of cytochrome P450 epoxygenase-derived eicosanoids. *Science* 285:1276–1279.
39. Wang Y, et al. (2005) Arachidonic acid epoxygenase metabolites stimulate endothelial cell growth and angiogenesis via mitogen-activated protein kinase and phosphatidylinositol 3-kinase/Akt signaling pathways. *J Pharmacol Exp Ther* 314:522–532.
40. Tesfamariam B, Brown ML, Cohen RA (1991) Elevated glucose impairs endothelium-dependent relaxation by activating protein kinase C. *J Clin Invest* 87:1643–1648.
41. Chien M-H, et al. (2009) Vascular endothelial growth factor-C (VEGF-C) promotes angiogenesis by induction of COX-2 in leukemic cells via the VEGF-R3/JNK/AP-1 pathway. *Carcinogenesis* 30:2005–2013.

BIOCHEMISTRY